

Strong-coupling theory for the thermodynamics of spin-1 planar magnetic chains

N. Papanicolaou and P. N. Spathis

Department of Physics, University of Crete, and Research Center of Crete, Heraklion, Greece

(Received 19 June 1995)

Earlier work on the $T=0$ dynamics of spin-1 chains with a strong easy-plane anisotropy is extended to include thermodynamics. Thus we carry out a systematic strong-coupling expansion to obtain analytical approximations for the spectrum of elementary excitations, the specific heat, and the magnetic susceptibility. Comparison with numerical data for the specific heat available in some important special cases indicates that our result is accurate for practically the entire temperature range. Similarly our calculation of the magnetic susceptibility reproduces to leading order a result obtained earlier through a molecular-field approximation and provides a definite improvement by including the two-loop correction. These theoretical predictions are directly relevant for a number of magnetic materials of current experimental interest.

I. INTRODUCTION

Antiferromagnetic spin-1 chains have attracted considerable attention in connection with the predicted Haldane gap in their spin-wave spectrum¹ which persists in the presence of a weak easy-plane anisotropy but is expected to vanish at some critical value of the anisotropy constant.² Nevertheless a gap of a different nature reappears above the critical value and is present in both antiferromagnetic (AFM) and ferromagnetic (FM) chains. Since there exist several experimental realizations of spin-1 chains with supercritical anisotropy^{3,4} the subject is of obvious theoretical interest.

The standard semiclassical theory of magnetism fails in the present problem, for it predicts no gap for either weak or strong easy-plane anisotropy. Alternative semiclassical theories specifically designed to address the strong-coupling phase^{5,6} capture the gross physical characteristics but also fail to provide an accurate description of important finer details. This situation prompted us to develop a strong-coupling expansion for the $T=0$ dynamics,⁷ in some respects superior to the available semiclassical methods.

Thus Ref. 7 provided analytical approximations for the dispersions of elementary excitations called excitons, which were later verified by a numerical diagonalization on finite chains.² We further predicted the occurrence of certain bound exciton states with the unusual property that they appear as sharp modes in the *two-point* longitudinal dynamic correlation function. Finally the exciton dispersions proved useful for a calculation of the specific heat at very low temperatures, within a dilute-exciton approximation, a result that was employed⁴ for the analysis of the observed specific heat in $\text{Ni}(\text{C}_2\text{H}_8\text{N}_2)_2\text{Ni}(\text{CN})_4$; to be referred to with the abbreviated symbol NENC.

The experimental work of Ref. 4 makes it clear that our earlier theoretical work⁷ needs to be extended in three ways. First, to provide a calculation of the specific heat that is valid beyond the low-temperature region. Second, to furnish a corresponding calculation of the magnetic susceptibility. Third, to include the effect of a small in-plane anisotropy that may be present in actual spin-1 chains. All three questions are addressed and answered affirmatively in the present paper.

In Sec. II we recalculate the spectrum of low-lying excitations for a general rhombic anisotropy. The strong-coupling

expansion is extended to thermodynamics in Secs. III and IV with an explicit computation of the specific heat and the magnetic susceptibility. In the concluding Sec. V we discuss potential applications of our theoretical results to systems of current experimental interest, whereas some of the lengthier calculational details are relegated to an Appendix.

II. ELEMENTARY EXCITATIONS

In this section we describe briefly an extension of the calculation of low-lying excitations⁷ to include the effect of a small in-plane anisotropy. Hence we consider spin-1 chains governed by the Hamiltonian

$$W = W_0 + W_1, \quad (2.1)$$

where W_0 accounts for the most general single-site anisotropy,

$$W_0 = \sum_{n=1}^N [A_1(S_n^1)^2 + A_2(S_n^2)^2 + A_3(S_n^3)^2], \quad (2.2)$$

and W_1 stands for the usual isotropic exchange interaction

$$W_1 = -J \sum_{n=1}^N (\mathbf{S}_n \cdot \mathbf{S}_{n+1}). \quad (2.3)$$

Actually the anisotropy constants present in Eq. (2.2) may be restricted according to

$$A_1 = E, \quad A_2 = -E, \quad A_3 = A, \quad (2.4)$$

without essential loss of generality thanks to the constraint $\mathbf{S}_n^2 = s(s+1) = 2$ satisfied by the spin operators. A more convenient set of independent parameters is given by

$$A, \quad \varepsilon = E/A, \quad \alpha = A/J, \quad (2.5)$$

where A sets the scale of energy, while ε and α are dimensionless.

The strong-coupling theory we are about to develop concerns spin chains whose dominant feature is a strong easy-plane anisotropy, i.e.,

$$A > 0, \quad |\varepsilon| < 1, \quad |\alpha| > 1, \quad (2.6)$$

and becomes increasingly accurate as the inequalities (2.6) become stronger. The exchange Hamiltonian W_1 will then be treated as a perturbation. One should note that the dimensionless parameters ε and α need not be positive. For example, α is positive for a ferromagnet ($J>0$) and negative for an antiferromagnet ($J<0$).

Since W_0 consists of a sum of mutually commuting operators, one for each site, its diagonalization is straightforward. For the moment we drop the site index and consider the vector basis

$$\begin{aligned} |1\rangle &= -\frac{1}{\sqrt{2}} [|1,1\rangle - |1,-1\rangle], \\ |2\rangle &= \frac{i}{\sqrt{2}} [|1,1\rangle + |1,-1\rangle], \quad |3\rangle = |1,0\rangle, \end{aligned} \quad (2.7)$$

where $|s,\mu\rangle$ are the elements of the familiar canonical basis with total spin $s=1$ and azimuthal spin $\mu=-1, 0$ or 1 . The action of the spin operators is given by

$$S^a |b\rangle = i \sum_c \varepsilon_{abc} |c\rangle, \quad (2.8)$$

where ε_{abc} is the usual antisymmetric tensor. An elementary calculation shows that the elements of the vector basis are eigenstates of W_0 ,

$$W_0 |1\rangle = \varepsilon_1 |1\rangle, \quad W_0 |2\rangle = \varepsilon_2 |2\rangle, \quad W_0 |3\rangle = \varepsilon_3 |3\rangle, \quad (2.9)$$

with eigenvalues

$$\varepsilon_1 = A(1-\varepsilon), \quad \varepsilon_2 = A(1+\varepsilon), \quad \varepsilon_3 = 0. \quad (2.10)$$

The fact that the eigenstates of W_0 given by Eq. (2.7) are independent of ε proved extremely helpful in all calculations presented in this paper.

We now return to the complete (periodic) chain with N sites and construct the low-lying eigenstates of W_0 . For $|\varepsilon|<1$, the ground state is given by

$$|\Omega_0\rangle = |3\rangle_1 \otimes |3\rangle_2 \cdots \otimes |3\rangle_N, \quad (2.11)$$

where $|3\rangle_n$ is the third element of the vector basis at site n . The ground state is nondegenerate and carries vanishing azimuthal spin ($\mu=0$) and vanishing energy ($\varepsilon_3=0$). Elementary excitations are obtained by exciting any single site in the chain to write

$$\begin{aligned} |x_n\rangle &= |3\rangle_1 \otimes |3\rangle_2 \cdots \otimes |1\rangle_n \cdots \otimes |3\rangle_N, \\ |y_n\rangle &= |3\rangle_1 \otimes |3\rangle_2 \cdots \otimes |2\rangle_n \cdots \otimes |3\rangle_N. \end{aligned} \quad (2.12)$$

There exist N independent states of type x_n , with $n=1, 2, \dots, N$, all with energy $\varepsilon_1=A(1-\varepsilon)$. Similarly there exist N independent states of type y_n with energy $\varepsilon_2=A(1+\varepsilon)$. This N -fold degeneracy is completely removed by considering states with definite crystal momentum k :

$$|x_k\rangle = \frac{1}{\sqrt{N}} \sum_n e^{-ikn} |x_n\rangle, \quad |y_k\rangle = \frac{1}{\sqrt{N}} \sum_n e^{-ikn} |y_n\rangle. \quad (2.13)$$

These are suitable linear superpositions of the excitons and antiexcitons of Ref. 7 and will be collectively referred to as

excitons. Note that the energy degeneracy of excitons and antiexcitons is lifted ($\varepsilon_1 \neq \varepsilon_2$) in the presence of an in-plane anisotropy ($\varepsilon \neq 0$).

Systematic corrections due to the exchange interaction may be obtained by standard perturbation theory. The absence of degeneracy in the zeroth-order ground state (2.11) and the exciton states (2.13) simplifies the calculation which will not be described here in any detail except to mention the useful identity

$$(\mathbf{S}_m \cdot \mathbf{S}_n) [|a\rangle_m \otimes |b\rangle_n] = [|b\rangle_m \otimes |a\rangle_n] - \delta_{ab} \sum_c [|c\rangle_m \otimes |c\rangle_n], \quad (2.14)$$

which is a consequence of Eq. (2.8). For $a \neq b$, $(\mathbf{S}_m \cdot \mathbf{S}_n)$ acts as an exchange operator.

An explicit third-order calculation yields the ground-state energy

$$W_{\text{gr}} = NA \left[w^{(0)} + \frac{w^{(1)}}{\alpha} + \frac{w^{(2)}}{\alpha^2} + \frac{w^{(3)}}{\alpha^3} + \cdots \right] \quad (2.15)$$

with

$$w^{(0)} = 0 = w^{(1)}, \quad w^{(2)} = -\frac{1}{1-\varepsilon^2}, \quad w^{(3)} = \frac{1}{2(1-\varepsilon^2)}. \quad (2.16)$$

Similarly the energy-momentum dispersions of the exciton modes read

$$\omega_{\pm}(k) = A \left[\omega^{(0)} + \frac{\omega^{(1)}}{\alpha} + \frac{\omega^{(2)}}{\alpha^2} + \frac{\omega^{(3)}}{\alpha^3} + \cdots \right] \quad (2.17)$$

with

$$\begin{aligned} \omega^{(0)} &= 1 \pm \varepsilon, \quad \omega^{(1)} = -2 \cos k, \\ \omega^{(2)} &= \frac{1}{1 \mp \varepsilon} + \frac{1 - \cos(2k)}{1 \pm \varepsilon}, \\ \omega^{(3)} &= \frac{\cos k}{2(1 \mp \varepsilon)^2} - \frac{1 - \cos(2k)}{1 - \varepsilon^2} + \frac{\cos k - \cos(3k)}{(1 \pm \varepsilon)^2}. \end{aligned} \quad (2.18)$$

At vanishing in-plane anisotropy ($\varepsilon=0$) the two exciton modes become degenerate ($\omega_+ = \omega_-$) and the preceding results reduce to the corresponding ones in Ref. 7. The accuracy of the predictions at $\varepsilon=0$ was discussed in detail in our earlier work and was later confirmed by a numerical diagonalization on finite chains.² The above discussions provide a guide for the domain of validity of our current results at small ε .

On the other hand, the perturbative spectrum is singular at $\varepsilon = \pm 1$ where level crossing occurs and one of the exciton modes becomes degenerate with the ground state. In fact, the nature of the ground state changes radically at $\varepsilon = \pm 1$ because the spin chain develops an *easy-axis* anisotropy with strength $D=2A$. The ground state is then strongly degenerate, in the limit $|D/J| \rightarrow \infty$, because spins may be assigned the azimuthal values ± 1 in any combination. As far as we can see such a strong degeneracy causes difficulties in the development of a successful strong-coupling theory and explains

the restriction $|\varepsilon| < 1$ present in Eq. (2.5). Actually, the stronger condition $|\varepsilon| \ll 1$ is required in order to obtain accurate predictions for reasonably large values of $|\alpha|$.

Returning to the easy-plane case we note that the process may be continued to multiexciton states constructed by exciting two or more sites in the chain. In particular, a new possibility arises with the formation of bound exciton states. A detailed discussion of such states was given in our earlier work⁷ in the absence of an in-plane anisotropy. We shall not attempt here to generalize the calculation of bound states to nonvanishing ε but turn to the main issue discussed in this paper; namely, the development of a strong-coupling theory for various thermodynamic quantities of practical interest.

III. SPECIFIC HEAT

The results of the preceding section provide some information on the low-temperature thermodynamics and were already used⁴ for the calculation of the specific heat in NENC. Specifically, a dilute-exciton approximation of the free energy is given by

$$F_{\text{exc}} = W_{\text{gr}} + NT \int_{-\pi}^{\pi} \frac{dk}{2\pi} [\ln(1 - e^{-\omega_+(k)/T}) + \ln(1 - e^{-\omega_-(k)/T})], \quad (3.1)$$

where W_{gr} is the ground-state energy of Eq. (2.15) and $\omega_{\pm}(k)$ are the exciton dispersions of Eq. (2.18). The corresponding specific heat (per site) reads

$$C_{\text{exc}} = -\frac{T}{N} \frac{\partial^2 F_{\text{exc}}}{\partial T^2} = \int_{-\pi}^{\pi} \frac{dk}{2\pi} \left[\left(\frac{\omega_+(k)/2T}{\sinh[\omega_+(k)/2T]} \right)^2 + \left(\frac{\omega_-(k)/2T}{\sinh[\omega_-(k)/2T]} \right)^2 \right]. \quad (3.2)$$

It should be noted that effects from the mutual interaction of excitons are neglected. In particular, there is no simple way to include the contribution of bound exciton states without overcounting. Hence the applicability of the dilute-exciton approximation is restricted to very low temperatures.

The main purpose of this paper is to derive a direct strong-coupling expansion of the free energy that includes effects from exciton interactions and is thus expected to be valid over a broad temperature range. The required formal machinery is contained in a classic paper of Schwinger.⁸ We are to calculate the partition function

$$Z = \text{tr } U(\beta), \quad U(\beta) = e^{-\beta(W_0 + W_1)}, \quad \beta = 1/T, \quad (3.3)$$

in a systematic strong-coupling expansion in which the exchange energy W_1 is treated as a perturbation. The zeroth-order approximation is given by

$$Z_0 = \text{tr } U_0(\beta), \quad U_0(\beta) = e^{-\beta W_0}, \quad (3.4)$$

and higher-order corrections may be derived from

$$U(\beta) = U_0(\beta) - \beta \int_0^1 dx U_0[(1-x)\beta] W_1 U_0(x\beta) + \beta^2 \int_0^1 x dx \int_0^1 dy U_0[(1-x)\beta] \times W_1 U_0[x(1-y)\beta] W_1 U_0(xy\beta) + \dots \quad (3.5)$$

This second-order approximation may be converted to a third-order one by using the identity

$$\text{tr } U(\beta) = \text{tr } U_0(\beta) - \beta \int_0^1 d\lambda \text{tr} [W_1 e^{-\beta(W_0 + \lambda W_1)}], \quad (3.6)$$

where we insert the expansion of $e^{-\beta(W_0 + \lambda W_1)}$ calculated from Eq. (3.5), with the substitution $W_1 \rightarrow \lambda W_1$, and perform the λ integration:

$$Z = \text{tr } U(\beta) = Z_0 + Z_1 + Z_2 + Z_3 + \dots, \\ Z_0 = \text{tr } U_0(\beta), \quad Z_1 = -\beta \text{tr} [W_1 U_0(\beta)], \\ Z_2 = \frac{1}{2} \beta^2 \int_0^1 dx \text{tr} \{W_1 U_0[(1-x)\beta] W_1 U_0(x\beta)\}, \\ Z_3 = -\frac{1}{3} \beta^3 \int_0^1 x dx \int_0^1 dy \text{tr} \{W_1 U_0[(1-x)\beta] \times W_1 U_0[x(1-y)\beta] W_1 U_0(xy\beta)\}, \quad (3.7)$$

and so on. These are the basic formal results that will be used in the following for a third-order calculation of the free energy and hence of the specific heat.

The zeroth-order approximation is simply

$$Z_0 = z_0^N, \quad z_0 = e^{-\beta\varepsilon_1} + e^{-\beta\varepsilon_2} + e^{-\beta\varepsilon_3}, \quad (3.8)$$

where ε_1 , ε_2 , and ε_3 are the eigenvalues (2.10). The calculation of traces in the higher-order corrections is, of course, easiest using the vector spin-1 basis (2.7) which diagonalizes the operators W_0 and $U_0 = e^{-\beta W_0}$. An important simplification results from the fact that the diagonal matrix elements of the spin operators vanish in the vector basis,

$$\langle b | S^a | b \rangle = 0, \quad (3.9)$$

as a consequence of Eq. (2.8). We may then immediately conclude that the first-order correction vanishes:

$$Z_1 = 0. \quad (3.10)$$

The second-order correction is written more explicitly as

$$Z_2 = \frac{1}{2} \beta^2 J^2 \sum_{mn} \int_0^1 dx \text{tr} \{ (\mathbf{S}_m \cdot \mathbf{S}_{m+1}) U_0[(1-x)\beta] \times (\mathbf{S}_n \cdot \mathbf{S}_{n+1}) U_0(x\beta) \}. \quad (3.11)$$

Because of Eq. (3.9) the only nonvanishing terms in the double sum are those with $m=n$ and they are all equal (n independent). Therefore,

$$Z_2 = \frac{1}{2} N \beta^2 J^2 z_0^{N-2} \int_0^1 dx \text{tr} \{ (\mathbf{S}_n \cdot \mathbf{S}_{n+1}) U_0[(1-x)\beta] \times (\mathbf{S}_n \cdot \mathbf{S}_{n+1}) U_0(x\beta) \}, \quad (3.12)$$

where the factor z_0^{N-2} originates in traces taken at sites other than n and $n+1$. The remaining trace involves spin operators at any two consecutive sites and may be computed by a repeated application of identity (2.14). One must also perform the x integration present in Eq. (3.12) to obtain after some lengthy algebra

$$\frac{Z_2}{Z_0} = \frac{N\beta^2 J^2}{2z_0^2} \left[z_0^2 - \sum_a e^{-2\beta\epsilon_a} - \sum_{a \neq b} \frac{e^{-2\beta\epsilon_a} - e^{-2\beta\epsilon_b}}{2\beta(\epsilon_a - \epsilon_b)} \right]. \quad (3.13)$$

The calculation of the third-order correction is similar in that a triple sum over the sites of the chain reduces to a simple sum where all spin operators involved are again defined over any two consecutive sites. We quote here the final result

$$\frac{Z_3}{Z_0} = -\frac{N\beta J^3}{6z_0^2} \sum_{a \neq b \neq c} \frac{e^{-2\beta\epsilon_a} - e^{-2\beta\epsilon_b}}{(\epsilon_a - \epsilon_b)(\epsilon_b - \epsilon_c)}. \quad (3.14)$$

Although calculation of higher-order terms appears feasible, we are content with the third-order result given above which will be analyzed in detail in the remainder of this section. In order to obtain completely explicit expressions we proceed as follows. First, we reorganize the expansion in terms of the free energy

$$F = -T \ln Z = -T [\ln Z_0 + (Z_2/Z_0) + (Z_3/Z_0) + \dots], \quad (3.15)$$

which agrees with Eq. (3.7) to third order because the first-order term vanishes ($Z_1=0$). Second, we insert in Eqs. (3.8), (3.13), and (3.14) the eigenvalues (2.10) and further use the dimensionless temperature

$$\tau = T/A, \quad \beta = 1/\tau, \quad (3.16)$$

noting that our current definition of the inverse temperature ($\beta=A/T$) differs from the one used earlier ($\beta=1/T$). Thus we write

$$F = N A f, \quad f = f^{(0)} + \frac{f^{(1)}}{\alpha} + \frac{f^{(2)}}{\alpha^2} + \frac{f^{(3)}}{\alpha^3} + \dots, \quad (3.17)$$

where the reduced free energy per site f is dimensionless and its strong-coupling coefficients are given by

$$z_0 \equiv 1 + 2e^{-\beta} \cosh(\epsilon\beta),$$

$$f^{(0)} = -\frac{1}{\beta} \ln z_0, \quad f^{(1)} = 0,$$

$$f^{(2)} = -\frac{1}{z_0^2} \left[\beta e^{-2\beta} + 2\beta e^{-\beta} \cosh(\epsilon\beta) + e^{-2\beta} \frac{\sinh(2\epsilon\beta)}{2\epsilon} + \frac{1 - e^{-2\beta} [\cosh(2\epsilon\beta) + \epsilon \sinh(2\epsilon\beta)]}{1 - \epsilon^2} \right],$$

$$f^{(3)} = \frac{1}{2(1 - \epsilon^2)z_0^2} \left[1 - e^{-2\beta} \cosh(2\epsilon\beta) - 2e^{-2\beta} \frac{\sinh(2\epsilon\beta)}{2\epsilon} \right]. \quad (3.18)$$

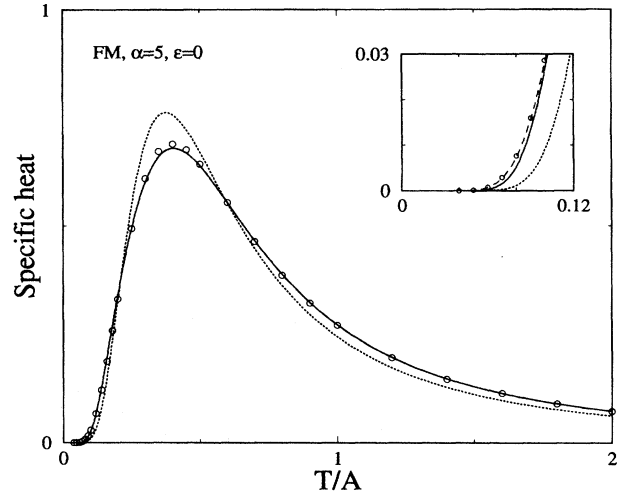


FIG. 1. Specific heat for a ferromagnetic spin-1 chain with $\alpha=A/J=5$ and vanishing in-plane anisotropy ($\epsilon=0$). Our third-order result is depicted by a solid line while the zeroth-order approximation is also displayed for comparison (dotted line). The circles stand for the numerical data of Blöte with their size chosen on purely aesthetic grounds. The inset concentrates on the low-temperature region where an even better agreement with the numerical data is obtained through the dilute-exciton approximation (3.2) (dashed line).

Simplifications occur in the limit of vanishing in-plane anisotropy where

$$\epsilon = 0, \quad u \equiv e^{-\beta} = e^{-1/\tau},$$

$$f^{(0)} = -\frac{1}{\beta} \ln(1 + 2u), \quad f^{(1)} = 0,$$

$$f^{(2)} = -\frac{(1+u)[1 + (2\beta-1)u]}{(1+2u)^2}, \quad f^{(3)} = \frac{1 - (2\beta+1)u^2}{2(1+2u)^2}. \quad (3.19)$$

The calculation of the specific heat is now straightforward using

$$C = -\frac{T}{N} \frac{\partial^2 F}{\partial T^2} = -\tau \frac{\partial^2 f}{\partial \tau^2}, \quad (3.20)$$

where we may insert the strong-coupling series for the free energy to obtain a corresponding series for the specific heat. The second derivative present in Eq. (3.20) can be computed analytically but leads to lengthy expressions. It is thus safer to work with the three-point formula

$$\frac{\partial^2 f}{\partial \tau^2} \approx \frac{1}{(\delta\tau)^2} [f(\tau + \delta\tau) + f(\tau - \delta\tau) - 2f(\tau)], \quad (3.21)$$

with $\delta\tau \sim 10^{-3}$, which proved to be more than adequate for all practical purposes.

In Fig. 1 we illustrate our main result for a uniaxial ($\epsilon=0$) FM chain with an intermediate easy-plane anisotropy $\alpha=A/J=5$ for which the specific heat was calculated numerically by Blöte.⁹ The observed overall agreement with the numerical data is satisfactory for practically the entire temperature

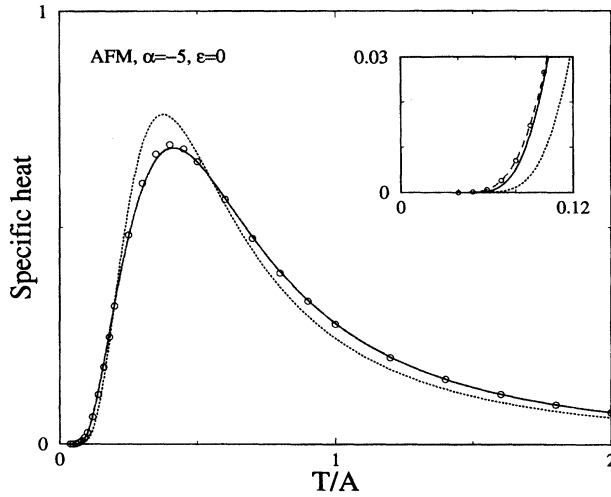


FIG. 2. An iteration of Fig. 1 for the corresponding antiferromagnetic chain with $\alpha=A/J=-5$. See the caption of Fig. 1 for further explanations.

range. A more detailed examination of the data reveals that the agreement improves rapidly at high temperatures. Nevertheless our third-order result performs well even at low temperatures, as is illustrated in the inset of Fig. 1. Yet a better agreement with the numerical data is obtained at very low temperatures by an indirect use of the strong-coupling expansion through the dilute-exciton approximation (3.2). But the direct strong-coupling expansion takes over decisively for temperatures greater than $T \sim 0.15A$ where the dilute-exciton approximation begins to deteriorate. In other words, $T \sim 0.15A$ is roughly the point at which exciton interactions become significant.

Before attempting a theoretical explanation of the preceding findings we proceed with some further illustrations. Thus in Fig. 2 we iterate Fig. 1 for the corresponding AFM chain. The overall picture remains the same. Actually it is difficult to discern at first sight any differences between the two figures because the calculated specific heat distinguishes a FM from an AFM chain only in the third-order correction which is small in this region of couplings ($|\alpha| \sim 5$). For even stronger anisotropy the difference becomes negligible. However a clear distinction between FM and AFM chains will emerge in the calculation of the magnetic susceptibility presented in Sec. IV.

It should be expected that the performance of our results will improve with increasing easy-plane anisotropy. Indeed the agreement with the numerical data obtained for an AFM chain with $\alpha = -10$ is excellent, as is shown in Fig. 3. Again, even better results are achieved at very low temperatures through the dilute-exciton approximation (3.2) but this point will not be discussed further in the present example.

Figures 2 and 3 taken in combination make it almost certain that our analytical results will prove accurate for the analysis of the measured specific heat of NENC throughout the temperature range. It should be noted that Ref. 4 assigns an anisotropy $\alpha = -7.5$ for which numerical results are not available. The calculated specific heat is plotted in Fig. 4 for both vanishing ($\epsilon = 0$) and a small ($\epsilon = 0.2$) in-plane anisot-

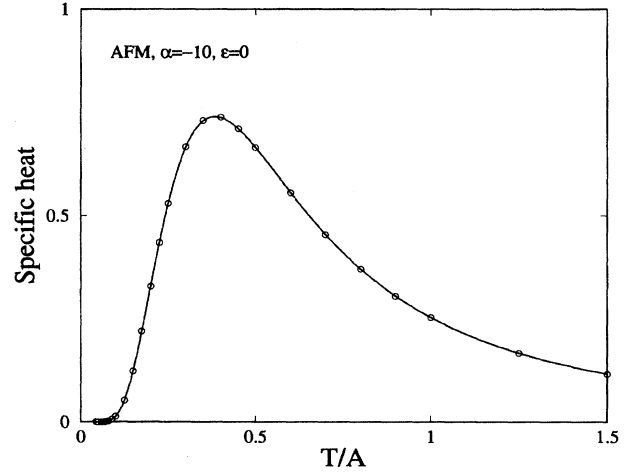


FIG. 3. Specific heat for an antiferromagnetic spin-1 chain with a strong easy-plane anisotropy $\alpha=A/J=-10$. The circles stand for the numerical data of Blöte.

ropy. In fact, the anticipated value of ϵ is smaller ($\epsilon \sim 0.1$) but we have chosen a larger value in our illustration in order to make the effect completely apparent. The in-plane anisotropy causes a depression of the specific heat around its maximum and an enhancement at low temperatures. The latter is partly explained by the softening of one of the exciton modes at nonvanishing ϵ . Therefore our analytical results may be used for a thorough analysis of the experimental data from NENC. In particular, one should be able to extract precise values for the parameters and eventually ascertain whether or not couplings other than those present in the model Hamiltonian are important.

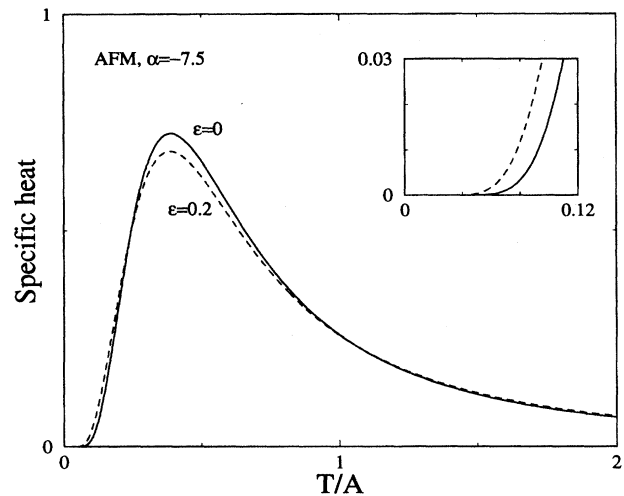


FIG. 4. Specific heat for an antiferromagnetic spin-1 chain with an easy-plane anisotropy $\alpha=A/J=-7.5$ appropriate for NENC. The solid line depicts our third-order result with vanishing in-plane anisotropy ($\epsilon=0$) and the dashed line is the same result with $\epsilon=0.2$. The inset concentrates on the low-temperature region where both curves are calculated from the dilute-exciton approximation (3.2) with $\epsilon=0$ and $\epsilon=0.2$.

For relatively low values of the easy-plane anisotropy, in the region $|\alpha| < 5$, the predictions of the strong-coupling series begin to gradually deteriorate. To be sure, the series diverges for $|\alpha| \sim 1$ where a phase transition takes place to a Haldane-like phase.² The numerical calculation of the above reference sets a practical lower bound for the validity of our exciton dispersions in the region $|\alpha| \sim 2.5$. Furthermore, Blöte⁹ gives numerical values for the specific heat also at $|\alpha| = 2.5$ which we compared with our analytical predictions; the deterioration of the strong-coupling series becomes apparent with the formation of a kinklike anomaly on the low-temperature (ascending) side of the specific heat. Therefore the current results may be applied for $|\alpha| > 2.5$ but with due caution at the lower end of this inequality. One should also recall the restriction on the in-plane anisotropy ($|\varepsilon| \ll 1$) discussed in the concluding paragraphs for Sec. II.

Finally we turn to some consistency checks that demonstrate in part both the correctness of our calculation and the reason for its success. In order to simplify matters the checks will be carried out at vanishing in-plane anisotropy ($\varepsilon = 0$) where the calculated free energy is given by Eq. (3.19).

First we address the high-temperature region where the agreement with the numerical data discussed earlier is generally very good. Now a high-temperature expansion of the specific heat calculated from Eqs. (3.19) and (3.20) reads

$$C = c_0 + c_1\beta + c_2\beta^2 + c_3\beta^3 + \dots, \quad \beta = A/T, \quad (3.22)$$

with

$$c_0 = 0 = c_1, \quad c_2 = \frac{2}{9} + \frac{4}{3\alpha^2}, \quad c_3 = \frac{2}{27} - \frac{2}{3\alpha^3}. \quad (3.23)$$

On the other hand, a direct high-temperature expansion based on the complete Hamiltonian reproduces the above results to third order whereas differences emerge starting with the coefficients c_4 . In general, the strong-coupling series carried to order n predicts correctly the first n coefficients of the high-temperature series. Such an instance explains the success of our results at high temperatures. But it should be stressed that the third-order result of the (direct) high-temperature expansion would perform rather poorly for most temperatures of practical interest.

In contrast, the strong-coupling series has been seen to perform well throughout the temperature range, especially when the dilute-exciton approximation is invoked to handle the region of very low temperatures. It is thus worth examining in some detail the low-temperature region where the calculated free energy (3.19) may be organized as an expansion in the exponentially small variable $u = e^{-\beta}$:

$$\begin{aligned} f_{\text{exc}}^{(0)} &= -\frac{2}{\beta}u + \frac{2}{\beta}u^2 + \dots, \quad f_{\text{exc}}^{(1)} = 0, \\ f_{\text{exc}}^{(2)} &= -1 - 2(\beta - 2)u + (6\beta - 11)u^2 + \dots, \\ f_{\text{exc}}^{(3)} &= \frac{1}{2} - 2u - \frac{1}{2}(2\beta - 11)u^2 + \dots. \end{aligned} \quad (3.24)$$

To appreciate the significance of the various terms in Eq. (3.24) we also consider the dilute-exciton approximation of the free energy given by Eq. (3.1), where we substitute for

the ground-state energy W_{gr} and the exciton dispersions $\omega_{\pm}(k)$ their strong-coupling approximations given by Eqs. (2.16) and (2.18) with $\varepsilon = 0$. We further organize the resulting expression as a double series in powers of $1/\alpha$ and $u = e^{-\beta}$. This step of the argument entails a large amount of algebra which will be omitted here. The analog of Eq. (3.24) is then given by

$$\begin{aligned} f_{\text{exc}}^{(0)} &= -\frac{2}{\beta}u - \frac{1}{\beta}u^2 + \dots, \quad f_{\text{exc}}^{(1)} = 0, \\ f_{\text{exc}}^{(2)} &= -1 - 2(\beta - 2)u - 4(\beta - 1)u^2 + \dots, \\ f_{\text{exc}}^{(3)} &= \frac{1}{2} - 2u - 4u^2 + \dots. \end{aligned} \quad (3.25)$$

The important observation is that zeroth-order as well as terms linear in $u = e^{-\beta}$ are the same in Eq. (3.24) and (3.25) but the coefficients of terms of order $u^2 = e^{-2\beta}$ and higher differ. The zeroth-order terms are just the strong-coupling coefficients $w^{(n)}$ of the ground-state energy (2.16), with $\varepsilon = 0$, as expected. One could also have anticipated that linear terms must be equal because they originate in single-exciton contributions which are free of interactions. Higher-order terms are sensitive to exciton interactions which are perturbatively included in the direct strong-coupling expansion but are completely absent from the dilute-exciton approximation. These observations touch upon the reason for the success of the direct expansion over a wide temperature range as well as for the observed relative superiority of the dilute-exciton approximation at very low temperatures; the latter being a selective and apparently more accurate resummation of all contributions that contain no interactions.

IV. MAGNETIC SUSCEPTIBILITY

Our third and final task is to study the effect of an applied magnetic field with an explicit calculation of the magnetic susceptibility. The strategy is the same as that of Sec. III except that the zeroth-order Hamiltonian is now extended according to

$$W_0 \rightarrow W_0 + \sum_n (\mathbf{h} \cdot \mathbf{S}_n), \quad \mathbf{h} \equiv g\mu_B \mathbf{H}, \quad (4.1)$$

where g is the gyromagnetic ratio and μ_B the Bohr magneton. We prefer to work with the reduced field \mathbf{h} reserving restoration of proper units for the end of the calculation. The direction of the applied field is also not specified for the moment:

$$\mathbf{h} = (h_1, h_2, h_3). \quad (4.2)$$

The elements of the vector basis (2.7) are no longer eigenstates of the zeroth-order Hamiltonian. The true eigenstates at each site may be written as linear superpositions of the form

$$|\mu\rangle = \sum_a C_a^\mu |a\rangle, \quad (4.3)$$

where the Latin index $a=1, 2$ or 3 counts the elements of the vector basis and the Greek index $\mu=1, 2$ or 3 the eigenstates. An elementary calculation shows that the (complex) amplitudes C_a^μ satisfy the linear system

$$\varepsilon_a C_a^\mu + i \sum_{bc} \varepsilon_{abc} h_b C_c^\mu = \lambda_\mu C_a^\mu, \quad (4.4)$$

applied for $a=1, 2$ and 3 . The new eigenvalues λ_μ with $\mu=1, 2$ or 3 reduce to those of Eq. (2.10) at vanishing field.

During the formal steps of the calculation we need not solve the eigenvalue problem (4.4) explicitly but may use the anticipated orthogonality relations

$$\sum_a \bar{C}_a^\mu C_a^\nu = \delta_{\mu\nu}, \quad \sum_\mu \bar{C}_a^\mu C_b^\mu = \delta_{ab}, \quad (4.5)$$

to express the free energy as a function of the eigenvalues λ_μ and the amplitudes

$$\Delta_{\mu\nu} = \sum_a C_a^\mu C_a^\nu, \quad \bar{\Delta}_{\mu\nu} = \sum_a \bar{C}_a^\mu \bar{C}_a^\nu, \quad (4.6)$$

where the bar denotes complex conjugation. It is important to note that the diagonal matrix elements of the spin operators in the new basis do not vanish,

$$\langle \mu | S^a | \mu \rangle = i \sum_{bc} \varepsilon_{abc} C_b^\mu \bar{C}_c^\mu, \quad (4.7)$$

in contrast to Eq. (3.9), and that the analog of identity (2.14) now reads

$$\begin{aligned} (\mathbf{S}_m \cdot \mathbf{S}_n) [| \mu \rangle_m \otimes | \nu \rangle_n] &= [| \nu \rangle_m \otimes | \mu \rangle_n] \\ &\quad - \Delta_{\mu\nu} \sum_{\sigma\rho} \bar{\Delta}_{\sigma\rho} [| \sigma \rangle_m \otimes | \rho \rangle_n]. \end{aligned} \quad (4.8)$$

Otherwise the calculation proceeds as in Sec. III. Thus we again apply the general formulas (3.7) to derive successive approximations of the partition function. The zeroth-order contribution reads

$$Z = z_0^N, \quad z_0 = e^{-\beta\lambda_1} + e^{-\beta\lambda_2} + e^{-\beta\lambda_3}, \quad (4.9)$$

while the first-order correction is now nonvanishing. Explicitly we write

$$\begin{aligned} Z_1 &= \beta J \sum_n \text{tr}[(\mathbf{S}_n \cdot \mathbf{S}_{n+1}) U_0(\beta)] \\ &= N \beta J z_0^{N-2} \text{tr}[(\mathbf{S}_n \cdot \mathbf{S}_{n+1}) U_0(\beta)]. \end{aligned} \quad (4.10)$$

In the second step of Eq. (4.10) the trace involves variables defined over any two consecutive sites and may easily be computed in the basis of eigenstates $|\mu\rangle$ discussed earlier. A straightforward application of identity (4.8) then yields

$$\frac{Z_1}{Z_0} = \frac{N\beta J}{z_0} \sum_{\mu\nu} (\delta_{\mu\nu} - \bar{\Delta}_{\mu\nu} \Delta_{\mu\nu}) e^{-\beta(\lambda_\mu + \lambda_\nu)}. \quad (4.11)$$

At vanishing field the amplitude $\Delta_{\mu\nu}$ reduces to the Kronecker delta ($\Delta_{\mu\nu} = \delta_{\mu\nu}$) and Z_1 vanishes, as expected. A sig-

nificant proliferation of terms occurs in the calculation of higher-order corrections. Nevertheless we have been able to also compute Z_2 which is listed in the Appendix and will be invoked here as the need arises.

We now proceed with an explicit calculation of the magnetic susceptibility. Consider first the case of a magnetic field applied along the first principal axis:

$$\mathbf{h} = (h_1, 0, 0). \quad (4.12)$$

Then the eigenvalues of system (4.4) are given by

$$\begin{aligned} \lambda_1 &= \varepsilon_1, \quad \lambda_2 = \frac{\varepsilon_2 + \varepsilon_3}{2} + \left[\left(\frac{\varepsilon_2 - \varepsilon_3}{2} \right)^2 + h_1^2 \right]^{1/2}, \\ \lambda_3 &= \frac{\varepsilon_2 + \varepsilon_3}{2} - \left[\left(\frac{\varepsilon_2 - \varepsilon_3}{2} \right)^2 + h_1^2 \right]^{1/2}, \end{aligned} \quad (4.13)$$

where $\varepsilon_1, \varepsilon_2$, and ε_3 are the zero-field eigenvalues (2.10). The corresponding eigenstates are determined from

$$C_1^1 = 1, \quad C_2^1 = 0, \quad C_3^1 = 0,$$

$$\begin{aligned} C_1^2 &= 0, \quad C_2^2 = \frac{h_1}{\sqrt{(\varepsilon_2 - \lambda_2)^2 + h_1^2}}, \quad C_3^2 = \frac{-i(\varepsilon_2 - \lambda_2)}{\sqrt{(\varepsilon_2 - \lambda_2)^2 + h_1^2}}, \\ C_1^3 &= 0, \quad C_2^3 = \frac{i(\varepsilon_3 - \lambda_3)}{\sqrt{(\varepsilon_3 - \lambda_3)^2 + h_1^2}}, \quad C_3^3 = \frac{h_1}{\sqrt{(\varepsilon_3 - \lambda_3)^2 + h_1^2}}, \end{aligned} \quad (4.14)$$

and the amplitudes $\Delta_{\mu\nu}$ may be computed by inserting Eq. (4.14) in Eq. (4.6). For our current purposes we shall need the above results only for a weak field where

$$\lambda_1 = \varepsilon_1, \quad \lambda_2 \approx \varepsilon_2 + \frac{h_1^2}{\varepsilon_2 - \varepsilon_3}, \quad \lambda_3 \approx \varepsilon_3 - \frac{h_1^2}{\varepsilon_2 - \varepsilon_3}, \quad (4.15)$$

and

$$(\Delta_{\mu\nu}) \approx \begin{pmatrix} 1 & 0 & 0 \\ 0 & 1 - \frac{1}{2} \delta^2 & i\delta \\ 0 & i\delta & 1 - \frac{1}{2} \delta^2 \end{pmatrix}; \quad \delta \equiv \frac{2h_1}{\varepsilon_2 - \varepsilon_3}. \quad (4.16)$$

Equations (4.15) and (4.16) summarize all information from the eigenvalue problem required for an explicit calculation of the magnetic susceptibility.

Specifically, let $F = F(h_1)$ be the free energy for a field with strength h_1 applied along the first principal axis. Then we consider the weak-field expansion

$$F(h_1) \approx F(0) - \frac{N}{2A} \chi_1 h_1^2 = F(0) - \frac{Ng^2 \mu_B^2}{2A} \chi_1 H_1^2 \quad (4.17)$$

and thus identify the corresponding susceptibility χ_1 . The various constants introduced in the right-hand side of Eq. (4.17) are such that χ_1 is dimensionless. More precisely, the calculated magnetic susceptibility is measured in units of

$$Ng^2 \mu_B^2 / A, \quad (4.18)$$

a convention that will be used in the following without exception.

Now the strong-coupling expansion of the free energy reads

$$F = -T \ln Z = -T \left[\ln Z_0 + (Z_1/Z_0) + \left((Z_2/Z_0) - \frac{1}{2} (Z_1/Z_0)^2 \right) + \dots \right], \quad (4.19)$$

where we have inserted the series $Z = Z_0 + Z_1 + Z_2 + \dots$ and consistently reexpanded to second order. Here Z_0 is given by Eq. (4.9), Z_1 by Eq. (4.11) and Z_2 by Eq. (A1) of the Appendix. Finally one must work out the weak-field expansion of the Z_i 's, through a systematic use of Eqs. (4.15) and (4.16), and eventually identify the susceptibility from Eq. (4.17). This step of the calculation is the lengthiest and will certainly not be described here. The final result may be written in the form

$$\chi_1 = \chi_1^{(0)} + \frac{1}{\alpha} \chi_1^{(1)} + \frac{1}{\alpha^2} \chi_1^{(2)} + \dots, \quad (4.20)$$

where

$$\begin{aligned} \chi_1^{(0)} &= -\frac{2A}{z_0} \frac{e^{-\beta\varepsilon_2} - e^{-\beta\varepsilon_3}}{\varepsilon_2 - \varepsilon_3}, \\ \chi_1^{(1)} &= \frac{8A^2}{z_0^2} \left(\frac{e^{-\beta\varepsilon_2} - e^{-\beta\varepsilon_3}}{\varepsilon_2 - \varepsilon_3} \right)^2 = 2[\chi_1^{(0)}]^2, \\ z_0 &\equiv e^{-\beta\varepsilon_1} + e^{-\beta\varepsilon_2} + e^{-\beta\varepsilon_3}, \end{aligned} \quad (4.21)$$

while the expression for $\chi_1^{(2)}$ is given in Eq. (A2) of the Appendix due to its considerable length. Note that we have restored in the above equations the zero-field definition of z_0 given earlier in Eq. (3.8). Hence the calculated susceptibility is expressed entirely in terms of the zero-field eigenvalues (2.10). We also note that the susceptibilities χ_2 and χ_3 along the second and third principal axis may be obtained from the preceding result by elementary cyclic permutations of the eigenvalues ε_1 , ε_2 , and ε_3 .

Therefore we have derived completely explicit expressions that can be used for the calculation of the susceptibilities for any value of the in-plane anisotropy ε . But the remainder of this section will be devoted to a detailed discussion only of the limit of vanishing ε where simpler forms can be derived. As expected, χ_1 and χ_2 are equal at $\varepsilon=0$. We may then use the more conventional notation

$$\chi_1 = \chi_2 \equiv \chi_{\perp}, \quad \chi_3 \equiv \chi_{\parallel} \quad (4.22)$$

for the transverse and the longitudinal susceptibility, respectively. At this point we also switch to the dimensionless inverse temperature $\beta = A/T$. The transverse susceptibility is given by

$$\chi_{\perp} = \chi_{\perp}^{(0)} + \frac{1}{\alpha} \chi_{\perp}^{(1)} + \frac{1}{\alpha^2} \chi_{\perp}^{(2)} + \dots, \quad (4.23)$$

with

$$\beta \equiv A/T, \quad u \equiv e^{-\beta},$$

$$\chi_{\perp}^{(0)} = \frac{2(1-u)}{1+2u}, \quad \chi_{\perp}^{(1)} = 2 \left[\frac{2(1-u)}{1+2u} \right]^2,$$

$$\begin{aligned} \chi_{\perp}^{(2)} &= \frac{1}{(1+2u)^3} [17 - (6\beta^2 + 4\beta + 30)u - (34\beta - 63)u^2 \\ &\quad - (16\beta + 50)u^3], \end{aligned} \quad (4.24)$$

and the longitudinal susceptibility by

$$\chi_{\parallel} = \chi_{\parallel}^{(0)} + \frac{1}{\alpha} \chi_{\parallel}^{(1)} + \frac{1}{\alpha^2} \chi_{\parallel}^{(2)} + \dots, \quad (4.25)$$

with

$$\chi_{\parallel}^{(0)} = \frac{2\beta u}{1+2u}, \quad \chi_{\parallel}^{(1)} = 2 \left(\frac{2\beta u}{1+2u} \right)^2,$$

$$\chi_{\parallel}^{(2)} = \frac{2\beta^2 u}{(1+2u)^3} [(\beta-2) + (8\beta+2)u^2]. \quad (4.26)$$

Some methodological remarks are in order. The transverse susceptibility was calculated from our basic relations (4.21) and (A2) applied with eigenvalues $\varepsilon_1 = A(1-\varepsilon)$, $\varepsilon_2 = A(1+\varepsilon)$, and $\varepsilon_3 = 0$. The longitudinal susceptibility was calculated from the *same* relations but with eigenvalues given by $\varepsilon_1 = 0$, $\varepsilon_2 = A(1-\varepsilon)$, and $\varepsilon_3 = A(1+\varepsilon)$, a choice that is equivalent to a two-step cyclic permutation. In both cases the limit $\varepsilon \rightarrow 0$ produced a large number of singular terms which all cancel against each other to yield the finite results (4.24) and (4.26). We interpret this extensive cancellation of singular terms as one of the numerous consistency checks to which we have subjected our calculation. A further check is provided by the observation that successive strong-coupling coefficients $\chi^{(n)}$, with $n=0,1,2,\dots$, behave at high temperatures as β^{n+1} for both susceptibilities, even though such a fact is not obvious at first sight in, say, $\chi_{\perp}^{(2)}$. This behavior is consistent with expectations based on a direct high-temperature expansion, in analogy with our related discussion of the specific heat.

The main results are illustrated in Fig. 5 for an AFM spin-1 chain with $\alpha = -7.5$ and $\varepsilon = 0$; i.e., for parameters that roughly describe NENC. The most conspicuous feature of this figure is that significant departures from the zeroth-order approximation occur at low temperatures for both the transverse and the longitudinal component. The latter is illustrated in greater detail in the inset of Fig. 5.

In the absence of numerical results for the magnetic susceptibility analogous to those available for the specific heat, at least in some important special cases, we must devise intrinsic checks in order to estimate the accuracy of our second-order predictions. As mentioned already, we expect our results to be increasingly accurate with increasing temperature. Thus we concentrate on the low-temperature region and examine first the longitudinal susceptibility for which a dilute-exciton approximation may easily be derived.

For a vanishing in-plane anisotropy and a field applied along the symmetry (third) axis the total (azimuthal) magnetization is a good quantum number. The ground state carries vanishing magnetization and suffers no energy shift due to the applied field; this fact explains the vanishing of the lon-

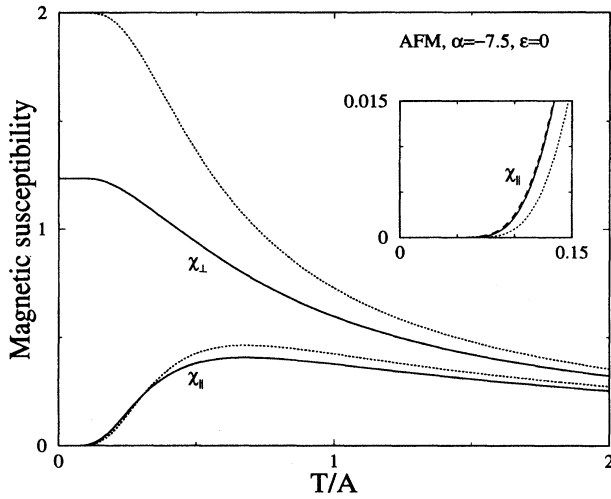


FIG. 5. Transverse (χ_{\perp}) and longitudinal (χ_{\parallel}) magnetic susceptibility for an antiferromagnetic spin-1 chain with $\alpha=A/J=-7.5$ and vanishing in-plane anisotropy ($\varepsilon=0$). Solid lines correspond to our second-order results of Eqs. (4.24) and (4.26), while the corresponding zeroth-order approximations are also displayed for comparison (dotted lines). The inset demonstrates the longitudinal susceptibility at low temperatures, with the prediction of the dilute-exciton approximation (4.29) added as a dashed line. All susceptibilities are measured in units of $Ng^2\mu_B^2/A$.

gitudinal susceptibility at $T=0$. On the other hand, excitons and antiexcitons⁷ carry a magnetization $+1$ and -1 , respectively, and thus undergo Zeeman splitting in their energy-momentum dispersions,

$$\omega_{\pm}(k) = \omega(k) \pm h, \quad (4.27)$$

where $\omega(k)$ is the common dispersion of excitons and antiexcitons at zero field. Note that (4.27) is an exact relation that makes no reference to a specific method of calculation of the basic dispersion $\omega(k)$. Now a dilute-exciton approximation of the free energy may be derived from Eq. (3.1) applied with ω_{\pm} given by Eq. (4.27):

$$F_{\text{exc}} = W_{\text{gr}} + NT \int_{-\pi}^{\pi} \frac{dk}{2\pi} [\ln(1 - e^{-\omega(k)/T} e^{-h/T}) + \ln(1 - e^{-\omega(k)/T} e^{h/T})]. \quad (4.28)$$

The only field dependence comes from the integral because the ground-state energy W_{gr} is independent of h . Expanding the integral in powers of h and using a relation analogous to Eq. (4.17) for the identification of the (dimensionless) longitudinal susceptibility we find that

$$\chi_{\parallel}^{\text{exc}} = \frac{A}{2T} \int_{-\pi}^{\pi} \frac{dk}{2\pi} \frac{1}{\sinh^2[\omega(k)/2T]}, \quad (4.29)$$

in units specified by Eq. (4.18).

Therefore we may apply Eq. (4.29) using our best (third-order) result for the exciton dispersion,

$$\omega(k) = A \left[1 - \frac{2}{\alpha} \cos k + \frac{1}{\alpha^2} (1 + 2 \sin^2 k) + \frac{1}{\alpha^3} \left[\frac{1}{2} (1 + 8 \sin^2 k) \cos k - 2 \sin^2 k \right] + \dots \right], \quad (4.30)$$

written here in a form given earlier in Ref. 7. Since this dispersion is expected to be very accurate for $|\alpha|=7.5$, the only uncertainty in applying Eq. (4.29) is the extent to which the dilute-exciton approximation is reasonable at finite temperatures. The result for $\alpha=-7.5$ is depicted in the inset of Fig. 5 together with the zeroth as well as the second-order approximation from the direct strong-coupling expansion. Interestingly, the emerging picture is very similar to the one encountered earlier in the discussion of the specific heat. Since it is reasonable to assume that the dilute-exciton approximation is accurate at very low temperatures also for the magnetic susceptibility, its close proximity to the second-order result of the direct expansion suggests that the latter is accurate also at low temperatures; of course, the direct expansion takes over decisively at higher temperatures.

The picture is slightly different for the transverse susceptibility which develops a nonvanishing value at $T=0$ where Eq. (4.24) gives

$$\chi_{\perp}(T=0) = 2 + \frac{8}{\alpha} + \frac{17}{\alpha^2} + \dots \quad (4.31)$$

A finite value at absolute zero is explained by the fact that the ground-state energy is a nontrivial function of the magnetic field when the latter is applied in the easy plane. Therefore the estimate (4.31) cannot be improved with any sort of a dilute-exciton approximation, but only with a third-order calculation within the direct strong-coupling expansion. Although we have not attempted such a calculation for the free energy, we have managed to obtain a third-order approximation of the ground-state energy W_{gr} using standard perturbation theory of the type discussed earlier in Sec. II. Once W_{gr} is computed as a function of the applied field, the $T=0$ susceptibility is calculated from a relation analogous to Eq. (4.17) with the free energy F replaced by W_{gr} . Thus we found that

$$\chi_{\perp}(T=0) = 2 + \frac{8}{\alpha} + \frac{17}{\alpha^2} + \frac{29}{\alpha^3} + \dots, \quad (4.32)$$

which reproduces Eq. (4.31) to second order, providing yet another check of consistency, but also leads to an improved (third-order) estimate of the $T=0$ transverse susceptibility. Applied for $\alpha=-7.5$ Eq. (4.31) yields $\chi_{\perp}(T=0)=1.24$, while Eq. (4.32) gives $\chi_{\perp}(T=0)=1.17$. The observed relative reduction of 6% may be taken as a rough estimate of the error. In other words, our second-order result is expected to *overestimate* the true transverse susceptibility by about 6% at

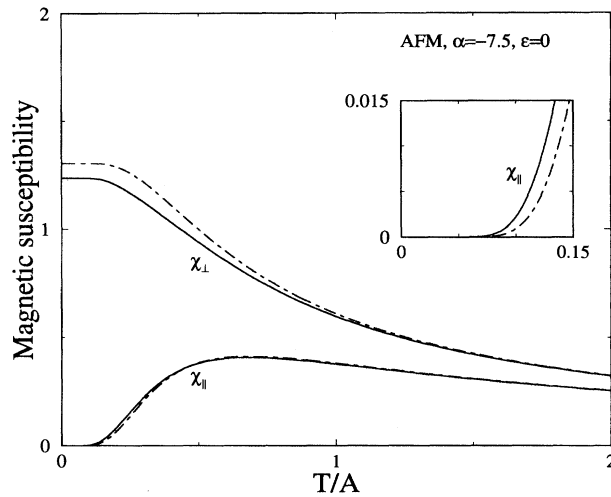


FIG. 6. Comparison of our second-order results for the magnetic susceptibilities (solid lines) with the predictions of the molecular-field approximation (4.33) for $\alpha=A/J=-7.5$ and vanishing in-plane anisotropy ($\epsilon=0$). The inset demonstrates the longitudinal susceptibility at low temperatures where the molecular-field approximation (broken line) is virtually identical with the corresponding zeroth-order approximation (the dotted line of Fig. 5). All susceptibilities are measured in units of $N g^2 \mu_B^2 / A$.

$T=0$, but the error is also expected to diminish quickly at finite temperatures.

As far as we know the only previous attempt to calculate the magnetic susceptibility beyond the zeroth order is the molecular-field approximation¹⁰

$$\chi_i \approx \frac{\chi_i^{(0)}}{1 - (2/\alpha)\chi_i^{(0)}}, \quad i=1,2, \text{ or } 3, \quad (4.33)$$

where χ_i is the susceptibility for a field applied along the i th principal axis and $\chi_i^{(0)}$ is its zeroth-order approximation. Expanding formula (4.33) in inverse powers of α leads to

$$\chi_i \approx \chi_i^{(0)} + \frac{2}{\alpha} [\chi_i^{(0)}]^2 + \frac{4}{\alpha^2} [\chi_i^{(0)}]^3 + \dots, \quad (4.34)$$

which agrees with the results of the systematic strong-coupling expansion to within the linear approximation given by Eq. (4.21) but disagrees with the quadratic approximation given by Eq. (A2). One might say that the molecular-field approximation is essentially a one-loop calculation cast in the form (4.33) obtained by a summation of some sort of ring diagrams, whereas our calculation includes up to two-loop effects exactly but makes no attempt to sum diagrams.

It is evident from the foregoing discussion that the molecular-field approximation cannot be used to provide an independent test of the accuracy of our results. But it is worth comparing the numerical predictions of Eq. (4.33) against our second-order calculation, as is done in Fig. 6. Although a rough overall agreement is obtained, significant differences arise in the low-temperature region especially for the longitudinal susceptibility for which the molecular-field prediction is virtually indistinguishable from the zeroth-order approximation (compare the inset of Fig. 6 with that of Fig.

5). The reason is simply that $\chi_{\parallel}^{(0)}$ behaves as $e^{-\beta}$ at low temperatures and the correction induced by the denominator of Eq. (4.33) is of order $e^{-2\beta}$. Furthermore the molecular-field approximation overestimates our second-order result for the transverse susceptibility at $T=0$, which in itself is an overestimate of the true transverse susceptibility. Therefore, while Eq. (4.33) provided a valuable first attempt to calculate the magnetic susceptibility,^{10,4} it is superseded by our present second-order calculation which should be used for a reanalysis of experimental data from, say, NENC.

We conclude this section with two comments. First, unlike the situation in the specific heat, the presence of a non-vanishing first-order correction in the magnetic susceptibility allows a clear distinction between AFM and FM spin-1 chains. For example, Eq. (4.32) gives the value $\chi_{\perp}(T=0)=1.17$ for an AFM chain with $\alpha=-7.5$, and the value $\chi_{\perp}(T=0)=3.44$ for the corresponding FM chain with $\alpha=7.5$. Second, the dependence of the magnetic susceptibility on the in-plane anisotropy ϵ is also linear, in contrast to the quadratic dependence of the specific heat, and should help to ascertain more definitely whether or not such an anisotropy is actually present.

V. CONCLUDING REMARKS

The work presented in this paper extends in an essential way our earlier calculation of the $T=0$ dynamics.⁷ We have thus developed a reasonably complete theoretical framework for spin-1 chains with a strong easy-plane anisotropy that can be directly applied to magnetic systems of current experimental interest.

Hence it is now clear that our calculation of elementary excitations (excitons and antiexcitons) is accurate for a wide range of parameters² and should provide a proper basis for the analysis of inelastic neutron-scattering experiments on CsFeBr_3 and CsFeCl_3 ; these are examples of an AFM and a FM spin-1 chain, respectively, with a supercritical easy-plane anisotropy.³ We have further predicted the occurrence of bound exciton states that should also be accessible to inelastic neutron scattering, but such states have not yet been observed.

The calculation of the thermodynamics given in the present paper was prompted by the experimental work on NENC (Ref. 4) and may in turn be used for a detailed reanalysis of the data. The range of validity of our theoretical results has been dealt with extensively in the main text and certainly includes the parameter range appropriate for NENC. In fact, this spin-1 system may well prove to be an ideal testing ground for the strong-coupling theory, provided that single crystals are grown which would allow a more detailed experimental work.

Finally we comment on possible future extensions of the strong-coupling theory. As is the case with all perturbative methods calculation of more terms in the strong-coupling series would certainly be welcome. Such a calculation may actually prove feasible thanks to the algebraic nature of the strong-coupling expansion. For the same reason, a generalization to higher-dimensional lattices, i.e., lattices with an arbitrary coordination number, should be straightforward.

ACKNOWLEDGMENTS

We are grateful to M. Orendac for communicating to us the experimental work of Ref. 4 and for a number of related discussions. The present work was supported in part by two grants from the EEC(SCI-CT-91-0705 and CHRX-CT93-0332).

APPENDIX

The purpose of this Appendix is merely to list some of the results pertinent to the calculation of the magnetic susceptibility that are too lengthy to include in the main text. Following closely the notation of Sec. IV we write for the second-order partition function

$$\begin{aligned} \frac{Z_2}{Z_0} = & \frac{N-3}{2N} \left(\frac{Z_1}{Z_0} \right)^2 + \frac{N\beta^2 J^2}{2z_0^2} \sum_{\mu\nu} \left[1 - 2\bar{\Delta}_{\mu\nu}\Delta_{\mu\nu} + \bar{\Delta}_{\mu\nu}\Delta_{\mu\nu} \sum_{\sigma\rho} \bar{\Delta}_{\sigma\rho}\Delta_{\sigma\rho} \frac{e^{\beta(\lambda_\mu+\lambda_\nu-\lambda_\sigma-\lambda_\rho)} - 1}{\beta(\lambda_\mu+\lambda_\nu-\lambda_\sigma-\lambda_\rho)} \right] e^{-\beta(\lambda_\mu+\lambda_\nu)} \\ & + \frac{N\beta^2 J^2}{z_0^3} \left[\sum_{\mu\nu} (\delta_{\mu\nu} - \bar{\Delta}_{\mu\nu}\Delta_{\mu\nu}) e^{-\beta(\lambda_\mu+2\lambda_\nu)} + \sum_{\mu\nu\sigma\rho} \bar{\Delta}_{\mu\nu}\Delta_{\mu\sigma}(\bar{\Delta}_{\sigma\rho}\Delta_{\nu\rho} - \delta_{\sigma\rho}\delta_{\nu\rho}) \frac{e^{\beta(\lambda_\nu-\lambda_\sigma)} - 1}{\beta(\lambda_\nu-\lambda_\sigma)} e^{-\beta(\lambda_\mu+\lambda_\nu+\lambda_\rho)} \right], \end{aligned} \quad (A1)$$

which should be supplemented with the stipulation that the function $(e^{\beta x} - 1)/\beta x$ be replaced by unity when $x=0$. The calculation of the second-order contribution to the magnetic susceptibility also follows the instructions of Sec. IV to yield the final result

$$\begin{aligned} \frac{\chi_1^{(2)}}{A^3} = & -\frac{16}{z_0^3} \left(\frac{e^{-\beta\varepsilon_2} - e^{-\beta\varepsilon_3}}{\varepsilon_2 - \varepsilon_3} \right)^3 - \frac{2\beta^2}{z_0^3} \frac{e^{-\beta\varepsilon_2} - e^{-\beta\varepsilon_3}}{\varepsilon_2 - \varepsilon_3} \left[\sum_{\mu} e^{-2\beta\varepsilon_\mu} + \sum_{\mu \neq \nu} \frac{e^{-2\beta\varepsilon_\mu} - e^{-2\beta\varepsilon_\nu}}{2\beta(\varepsilon_\mu - \varepsilon_\nu)} \right] + \frac{1}{z_0^2} \left[2\beta^2 \frac{e^{-2\beta\varepsilon_2} - e^{-2\beta\varepsilon_3}}{\varepsilon_2 - \varepsilon_3} \right. \\ & + 2\beta \frac{e^{-2\beta\varepsilon_2} + e^{-2\beta\varepsilon_3} - 8e^{-\beta(\varepsilon_2+\varepsilon_3)}}{(\varepsilon_2 - \varepsilon_3)^2} - \frac{1}{(\varepsilon_1 - \varepsilon_2)(\varepsilon_2 - \varepsilon_3)} \left(2\beta e^{-2\beta\varepsilon_2} + \frac{e^{-2\beta\varepsilon_1} - e^{-2\beta\varepsilon_2}}{\varepsilon_1 - \varepsilon_2} \right) \\ & + \frac{1}{(\varepsilon_1 - \varepsilon_3)(\varepsilon_2 - \varepsilon_3)} \left(2\beta e^{-2\beta\varepsilon_3} + \frac{e^{-2\beta\varepsilon_1} - e^{-2\beta\varepsilon_3}}{\varepsilon_1 - \varepsilon_3} \right) + \frac{4}{(\varepsilon_2 - \varepsilon_3)^2} \left(\frac{e^{-2\beta\varepsilon_1} - e^{-2\beta\varepsilon_2}}{\varepsilon_1 - \varepsilon_2} + \frac{e^{-2\beta\varepsilon_1} - e^{-2\beta\varepsilon_3}}{\varepsilon_1 - \varepsilon_3} \right) \\ & \left. - 6 \frac{e^{-2\beta\varepsilon_2} - e^{-2\beta\varepsilon_3}}{(\varepsilon_2 - \varepsilon_3)^3} - 16 \frac{e^{-2\beta\varepsilon_1} - e^{-\beta(\varepsilon_2+\varepsilon_3)}}{(\varepsilon_2 - \varepsilon_3)^2(2\varepsilon_1 - \varepsilon_2 - \varepsilon_3)} \right]. \end{aligned} \quad (A2)$$

Here $\beta=1/T$ and we have restored the zero-field definition of z_0 , namely

$$z_0 = e^{-\beta\varepsilon_1} + e^{-\beta\varepsilon_2} + e^{-\beta\varepsilon_3}. \quad (A3)$$

In spite of its considerable length relation (A2) is completely explicit and can be used together with Eqs. (4.21) for a calculation of the susceptibility χ_1 simply by inserting the eigenvalues $\varepsilon_1=A(1-\varepsilon)$, $\varepsilon_2=A(1+\varepsilon)$, and $\varepsilon_3=0$ of Eq. (2.10). The susceptibility χ_2 can be computed from the *same* basic relations applied for $\varepsilon_1=A(1+\varepsilon)$, $\varepsilon_2=0$, and $\varepsilon_3=A(1-\varepsilon)$, and χ_3 for $\varepsilon_1=0$, $\varepsilon_2=A(1-\varepsilon)$, and $\varepsilon_3=A(1+\varepsilon)$.

¹F. D. M. Haldane, Phys. Lett. A **93**, 464 (1983); J. Appl. Phys. **57**, 3359 (1985).

²O. Golinelli, Th. Jolicœur, and R. Lacage, Phys. Rev. B **46**, 10 854 (1992).

³B. Schmid, B. Dorner, D. Visser, and M. Steiner, Z. Phys. B **86**, 257 (1992).

⁴M. Orendac *et al.*, J. Magn. Magn. Mater. **140-144**, 1643 (1995); Phys. Rev. B **52**, 3435 (1995).

⁵P. A. Lindgard, Physica B **120**, 190 (1983).

⁶N. Papanicolaou, Nucl. Phys. B **240**, 281 (1984); **305**, 386 (1988).

⁷N. Papanicolaou and P. Spathis, J. Phys. Condens. Matter **1**, 5555 (1989); **2**, 6575 (1990).

⁸J. Schwinger, Phys. Rev. **82**, 664 (1951).

⁹H. W. J. Blöte, Physica B **79**, 427 (1975).

¹⁰R. L. Carlin, C. T. O'Connor, and S. N. Bhatia, J. Am. Chem. Soc. **98**, 3523 (1976).